13

Computation of reconstruction kernels

This chapter is concerned with the computation of a reconstruction kernel associated with $\bar{e}_\gamma$, where the calculations are performed in detail for the mollifier given by (12.3), (12.5), (12.20) and (12.21). Our aim is to find a representation of

$$\bar{\upsilon}_\gamma = \mathsf{E}\bar{e}_\gamma \,. \tag{13.1}$$

The reconstruction kernel corresponding to $e_\gamma(x,y) = \mathcal{T}^y_{\mathrm{e},M}\bar{e}_\gamma(x)$ is then $\upsilon_\gamma(y) = \mathcal{G}^y_{\mathrm{r},M}\bar{\upsilon}_\gamma$ according to Corollary 11.7. From Lemma 11.5, we read that

$$\mathbf{F}\bar{\upsilon}_\gamma(\sigma,\varrho) = \mathbf{F}\,\mathsf{E}\bar{e}_\gamma(\sigma,\varrho) = \mathbf{F}\bar{e}_\gamma(\sigma, \sqrt{\varrho^2 - \|\sigma\|^2})\,, \tag{13.2}$$

when $\varrho \geq \|\sigma\|$, $\varrho \geq 0$ and $\sigma \in \mathbb{R}^n$. First, we have to calculate the Fourier transform of $\bar{e}_\gamma$.

Lemma 13.1. *We have*

$$\mathbf{F}\bar{e}_\gamma(\sigma,\varrho) = \hat{\bar{e}}_\gamma(\sigma,\varrho) = \hat{\bar{e}}^1_\gamma(\sigma)\,\hat{\bar{e}}^2_\gamma(\varrho) = \cos(\varrho)\,\mathrm{e}^{-\gamma^2\,\|\sigma\|^2/2}\,\mathrm{e}^{-\gamma^4\,\varrho^4} \tag{13.3}$$

for $\sigma \in \mathbb{R}^n$, $\varrho \in \mathbb{R}$.

Proof. Because of $\hat{\bar{e}}^1_\gamma(\sigma) = \mathrm{e}^{-\gamma^2\,\|\sigma\|^2/2}$ equation (13.3) follows from

$$\begin{aligned}
\hat{\bar{e}}^2_\gamma(\varrho) &= \frac{1}{2\,\gamma}\int_{\mathbb{R}}\Big\{F\Big(\frac{q+1}{\gamma}\Big) + F\Big(\frac{q-1}{\gamma}\Big)\Big\}\,\mathrm{e}^{-\imath\,q\,\varrho}\,\mathrm{d}q \\
&= \frac{1}{2}\,(\mathrm{e}^{\imath\,\varrho} + \mathrm{e}^{-\imath\,\varrho})\int_{\mathbb{R}} F(q)\,\mathrm{e}^{-\imath\,\gamma\,q\,\varrho}\,\mathrm{d}q \\
&= \cos(\varrho)\,\mathrm{e}^{-(\gamma\,\varrho/2)^4}\,.
\end{aligned}$$

$\square$

For $\varrho \geq \|\sigma\|$, we deduce

$$\mathbf{F}\bar{\upsilon}_\gamma(\sigma,\varrho) = \cos(\sqrt{\varrho^2 - \|\sigma\|^2})\,\mathrm{e}^{-\gamma^2\,\|\sigma\|^2/2}\,\mathrm{e}^{-\gamma^4\,(\varrho^2 - \|\sigma\|^2)^2/16}\,. \tag{13.4}$$

from Lemma 13.1 and (13.2). With the help of (13.4), we see that an extension of $\hat{\bar{v}}_\gamma$ to the whole of $\mathbb{R}^n \times [0, \infty)$ as a function from $\mathcal{S}_\mathrm{r}$ requires an extension of $\cos(\sqrt{\xi})$ for $\xi < 0$. Thus, we need a function $G \in \mathcal{C}^\infty(\mathbb{R})$ with $G(\xi) = \cos(\sqrt{\xi})$, if $\xi \geq 0$, such that

$$\mathbf{F}\bar{v}_\gamma(\sigma, \varrho) = G(\varrho^2 - \|\sigma\|^2)\, \mathrm{e}^{-\gamma^2\, \|\sigma\|^2/2} \mathrm{e}^{-\gamma^4\, (\varrho^2 - \|\sigma\|^2)^2/16} \tag{13.5}$$

is meaningfully defined for *all* $\sigma \in \mathbb{R}^n$, $\varrho \geq 0$ and additionally is a function in $\mathcal{S}_\mathrm{r}$. The latter one implies that $\bar{v}_\gamma \in \mathcal{S}_\mathrm{r}$.

The first idea to extend $\cos(\sqrt{\xi})$ is to use its power series expansion. For $\xi \geq 0$ we have

$$\cos(\sqrt{\xi}) = \sum_{k=0}^{\infty} \frac{(-1)^k}{2\,k!}\, \xi^k\,. \tag{13.6}$$

Using the power series (13.6) to extend $\cos(\sqrt{\xi})$ on $\xi < 0$ we obtain the function

$$G(\xi) = \begin{cases} \cos(\sqrt{\xi})\,, & \xi \geq 0\,, \\ \cosh(\sqrt{|\xi|})\,, & \xi < 0 \end{cases}$$

which obviously is in $\mathcal{C}^\infty(\mathbb{R})$, but unbounded. If we take into account that $G(\xi) = \mathcal{O}(\exp(\sqrt{|\xi|}))$ for $\xi \to -\infty$, then in fact we have that $\mathbf{F}\bar{v}_\gamma \in \mathcal{S}_\mathrm{r}$.

As outlined in Remark 11.9 the particular choice of the extension for $\mathbf{F}\bar{v}_\gamma$ on $0 \leq \varrho < \|\sigma\|$ has no impact to $\widetilde{\mathbf{M}}_\gamma\,\mathbf{M}f$, since $\operatorname{supp}\mathbf{F}\,\mathbf{M}f \subset \{(\sigma, \varrho) : \varrho \geq \|\sigma\|\}$. In applications, we only have a finite number of data available as it was expressed by equation (11.23). This implies that the data are given on a bounded domain $(z, r) \in Z_N \times [0, R]$ only, where $Z_N \subset \mathbb{R}^n$ is bounded and $R > 0$. As a consequence, the specific extension of G actually has an influence to $\widetilde{\mathbf{M}}_{N,\gamma}\,\mathbf{M}f$. Numerical tests have shown that a bounded $G(\xi) \in \mathcal{C}(\mathbb{R})$ is desirable. To this end, we introduce a cut-off function $\chi \in \mathcal{C}^\infty(\mathbb{R})$ which is supposed to have the properties

$$\begin{aligned} \chi(\xi) &= 1\,, \quad \text{if } \xi \geq 0\,, \\ \chi(\xi) &= 0\,, \quad \text{if } \xi < -1\,, \\ \chi^{(k)}(-1) = \chi^{(k)}(0) &= 0\,, \quad \text{for all } k \geq 1\,. \end{aligned}$$

Such a function is explicitly given by

$$\chi(\xi) = \frac{u(\xi+1)}{u(\xi+1) + u(-\xi)}\,,$$

where

$$u(\xi) = \begin{cases} \mathrm{e}^{-1/\xi}\,, & \xi > 0\,, \\ 0\,, & \xi \leq 0 \end{cases}$$

The bounded extension $\widetilde{G}$ of $\cos(\sqrt{\xi})$ finally reads as

$$\widetilde{G}(\xi) = \begin{cases} \cos(\sqrt{\xi})\,, & \xi \geq 0\,, \\ \chi(\xi)\,\cosh(\sqrt{|\xi|})\,, & \xi < 0 \end{cases} \tag{13.7}$$

and is a bounded function in $\mathcal{C}^\infty(\mathbb{R})$. Plots of χ as well as of the extension $\widetilde{G}$ are displayed in Figure 13.1.

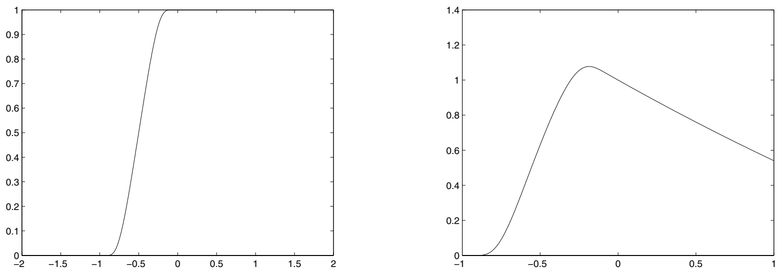

Fig. 13.1. Plots of the cut-off function χ (left picture) and the extension $\widetilde{G}$ (right picture). We have displayed $\widetilde{G}(\xi)$ only in the interval $\xi \in [-1, 1]$ to emphasize the smoothness of the extension.

The reconstruction kernel $\bar{\upsilon}_\gamma$ is now computed applying the inverse Fourier transform to (13.5).

Lemma 13.2. *Let* $\bar{e}_\gamma = \bar{e}^1_\gamma \otimes \bar{e}^2_\gamma$ *be given by* (12.5), (12.20) *and* (12.21). *Then a solution of*

$$\mathbf{M}^* \bar{\upsilon}_\gamma = \bar{e}_\gamma$$

is represented by

$$\bar{\upsilon}_\gamma(z,r) = \frac{1}{2\,\pi^2} \int_0^\infty \int_0^\infty \Big\{ \widetilde{G}(\varrho^2 - \sigma^2)\, \mathrm{e}^{-\gamma^2\,(\frac{\sigma^2}{2} + \gamma^2\,(\varrho^2-\sigma^2)^2/16)} \times \varrho\,\mathrm{J}_0(\varrho\, r)\, \cos(\sigma\, z) \Big\}\, \mathrm{d}\varrho\, \mathrm{d}\sigma \quad \textit{for } n = 1\,, \tag{13.8a}$$

$$\bar{\upsilon}_\gamma(z,r) = (2\,\pi)^{-n-\frac{1}{2}}\, r^{(1-n)/2}\, t^{(2-n)/2} \times \int_0^\infty \int_0^\infty \Big\{ \widetilde{G}(\varrho^2 - \tau^2)\, \mathrm{e}^{-\gamma^2\,(\frac{\tau^2}{2} + \gamma^2\,(\varrho^2-\tau^2)^2/16)} \times \varrho^{(n+1)/2}\, \tau^{(2-n)/2}\, \mathrm{J}_{(n-1)/2}(\varrho\, r)\, \mathrm{J}_{(n-2)/2}(\tau\, t) \Big\}\, \mathrm{d}\varrho\, \mathrm{d}\tau \quad \textit{for } n > 1\,. \tag{13.8b}$$

Here $r, t > 0$, J_ν *denotes the Bessel function of first kind of order* ν *and* $\widetilde{G}$ *is defined as in* (13.7). *In* (13.8b) *we have* $t = \|z\|$ *and* $\tau = \|\sigma\|$.

Proof. Formulas (13.8a), (13.8b) follow from (13.5) by an application of the $(2n+1)$-dimensional inverse Fourier transform and using identity (13.3) and spherical coordinates. The proof is completed with the help of

$$\int_{S^n} \mathrm{e}^{\imath\, \varrho\, r\, \langle \omega, \theta \rangle}\, \mathrm{d}S_n(\omega) = (2\,\pi)^{(n+1)/2}\, (\varrho\, r)^{(1-n)/2}\, \mathrm{J}_{(n-1)/2}(\varrho\, r)\,,$$

which is found e.g. in FAWCETT [30]. □

Since the σ-variable is in $\mathbb{R}$ if $n = 1$, the introduction of spherical coordinates for the integration with respect to σ does not make sense in that case. That is why we wrote down the representation of $\bar{\upsilon}_\gamma(z, r)$ for $n = 1$ separately. The kernel $\bar{\upsilon}_\gamma$ is illustrated in Figure 13.2 for $\gamma = 0.06$ and $n = 1$, i.e. the two-dimensional setting. The integrals in (13.8a) were computed by numerical integration where we confined to values (σ, ϱ) for which the integrand is greater than or equal to 10^{-12}. The reconstruction kernel plotted in Figure 13.2 is associated with the mollifier $\bar{e}_\gamma$ and also reaches its global maximum at $(0, 1)$. This again is compatible with the group structure which underlies the operators $\mathcal{G}^y_{\mathrm{r},M}$.

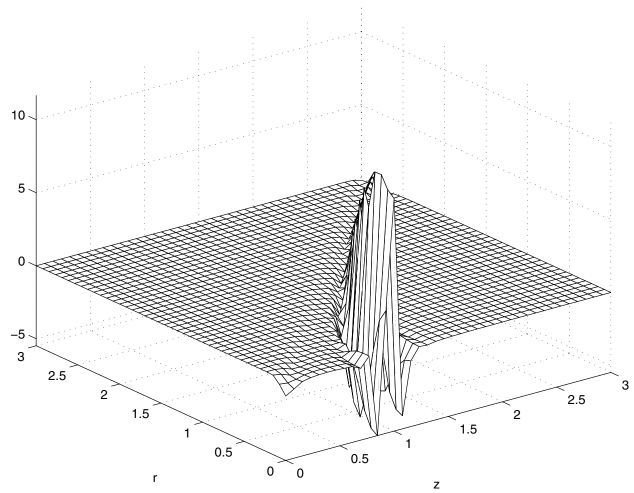

Fig. 13.2. The reconstruction kernel $\bar{\upsilon}_\gamma$ given as in (13.8a) for $\gamma = 0.06$ and $n = 1$. A cross section through the z-axis again would show the similarity to the Shepp-Logan filter just as in Doppler tomography, compare Figure 7.35, whereas we have a smoothing with respect to the radius variable r.

The computation of the reconstruction kernel corresponding to the mollifier with compactly supported Fourier transform is done accordingly.

Corollary 13.3. *If the mollifier* $\bar{e}_\gamma = \bar{e}^1_\gamma \otimes \bar{e}^2_\gamma$ *is defined by* (12.4), (12.5), (12.22) *and* (12.23), *then a corresponding reconstruction kernel can be written as*

$$\bar{\upsilon}_\gamma(z,r) =$$

$$\frac{1}{2\,\pi^2}\Big\{ \int_0^{\gamma^{-1}} \int_0^{\gamma^{-1}} \eta\, \mathrm{J}_0(\sqrt{\eta^2+\sigma^2}\,r)\, \cos\eta\, \mathrm{e}^{2-\frac{\gamma^2\,(\sigma^2-\gamma^2\,\eta^4)}{(1-\gamma^2\,\sigma^2)\,(1-\gamma^4\,\sigma^4)}}\, \cos(\sigma\,z)\,\mathrm{d}\eta\,\mathrm{d}\sigma$$

$$+ \int_0^{\gamma^{-1}} \int_0^{\sigma} \eta\, \mathrm{J}_0(\sqrt{\sigma^2-\eta^2}\,r)\,\chi(-\eta^2)\, \cosh\eta\, \mathrm{e}^{2-\frac{\gamma^2\,(\sigma^2-\gamma^2\,\eta^4)}{(1-\gamma^2\,\sigma^2)\,(1-\gamma^4\,\sigma^4)}}\, \cos(\sigma\,z)\,\mathrm{d}\eta\,\mathrm{d}\sigma\Big\}$$

for $n = 1$, $z \in \mathbb{R}$, $r \geq 0$ *and*

$$\bar{\upsilon}_\gamma(z,r) = (2\,\pi)^{-n-\frac{1}{2}}\, r^{(1-n)/2}\, t^{(2-n)/2}$$

$$\times\Big\{ \int_0^{\gamma^{-1}} \int_0^{\gamma^{-1}} \eta\, \mathrm{J}_{\frac{n-1}{2}}(\sqrt{\eta^2+\tau^2}\,r)\, \cos\eta\, \mathrm{e}^{2-\frac{\gamma^2\,(\tau^2-\gamma^2\,\eta^4)}{(1-\gamma^2\,\tau^2)\,(1-\gamma^4\,\tau^4)}}\, \mathrm{J}_{\frac{n-2}{2}}(\tau\,t)\,\mathrm{d}\eta\,\mathrm{d}\tau +$$

$$+ \int_0^{\gamma^{-1}} \int_0^{\tau} \eta\, \mathrm{J}_{\frac{n-1}{2}}(\sqrt{\tau^2-\eta^2}\,r)\,\chi(-\eta^2)\, \cosh\eta\, \mathrm{e}^{2-\frac{\gamma^2\,(\tau^2-\gamma^2\,\eta^4)}{(1-\gamma^2\,\tau^2)\,(1-\gamma^4\,\tau^4)}}\, \mathrm{J}_{\frac{n-2}{2}}(\tau\,t)\,\mathrm{d}\eta\,\mathrm{d}\tau\Big\}$$

for $n > 1$, $t = \|z\|$, $\tau = \|\sigma\|$, *and* $r \geq 0$.

In Corollary 13.3, we additionally applied substitutions $\varrho = \sqrt{\eta^2+\sigma^2}$ and $\varrho = \sqrt{\sigma^2-\eta^2}$. Note that we do not need to restrict the integration limits in order to apply numerical integration since they are finite.